mathematics

MDPI

Article

Accurate Key Parameters Estimation of PEMFCs' Models Based on Dandelion Optimization Algorithm

Rabeh Abbassi [1,2,3,*], Salem Saidi [2,4], Abdelkader Abbassi [3,5], Houssem Jerbi [6], Mourad Kchaou [1] and Bilal Naji Alhasnawi [7]

[1] Department of Electrical Engineering, College of Engineering, University of Ha'il, Ha'il City 81451, Saudi Arabia
[2] LaTICE Laboratory, Higher National Engineering School of Tunis (ENSIT), University of Tunis, 5 Avenue Taha Hussein, P.O. Box 56, Tunis 1008, Tunisia
[3] Institute of Applied Sciences and Technology of Kasserine (ISSATKas), University of Kairouan, P.O. Box 471, Kasserine 1200, Tunisia
[4] National School of Advanced Sciences and Technologies of Borj Cédria (ENSTAB), University of Carthage, P.O. Box 122, Hammam-Chott 1164, Tunisia
[5] Engineering Laboratory of Industrial Systems and Renewable Energies (LISIER), National Higher Engineering School of Tunis (ENSIT), University of Tunis, 5 Avenue Taha Hussein, P.O. Box 56, Tunis 1008, Tunisia
[6] Department of Industrial Engineering, College of Engineering, University of Ha'il, Ha'il City 81451, Saudi Arabia
[7] Department of Computer Technical Engineering, College of Information Technology, Imam Ja'afar Al-Sadiq University, Al-Muthanna 66002, Iraq
* Correspondence: r.abbassi@uoh.edu.sa

Abstract: With the increasing demand for electrical energy and the challenges related to its production, along with the need to be environmentally friendly to achieve sustainability for future generations, proton exchange membrane fuel cells (PEMFCs) are emerging as a clean energy source that can effectively replace conventional energy sources, in various fields of application and especially in the field of transportation exploiting electric vehicles (EVs). To improve the development and control of the PEMFCs, the precise determination of its mathematical model remains an essential task. Indeed, the accuracy of such a model depends on the ability to overcome the constraints associated with the nonlinearity and the numerous involved unknown parameters. The present paper proposes a new Dandelion Optimizer (DO) to accurately identify, for the first time, the parameters of the PEMFC model. The DO addresses the weaknesses of the majority of metaheuristic algorithms related to the self-adaptation of parameters, the stagnation of convergence to local minima, and the ability to refer to the whole population. The high ability of the proposed method is investigated using both steady-state and dynamic situations. The DO-based parameters estimation approach has been assessed through a specific comparative study with the most recently published techniques including GWO, GBO, HHO, IAEO, VSDE, and ABCDESC is performed using two typical PEMFC modules, namely 250 W PEMFC and NedStack PS6. The results obtained proved that the proposed approach obtained promising achievements and better performances comparatively with well-recognized and competitive methods.

Keywords: proton exchange membrane fuel cell; key parameters estimation; Hail region desert tourism; sum of square error; electric circuit model; dandelion optimization algorithm

MSC: 35Q93

Citation: Abbassi, R.; Saidi, S.; Abbassi, A.; Jerbi, H.; Kchaou, M.; Alhasnawi, B.N. Accurate Key Parameters Estimation of PEMFCs' Models Based on Dandelion Optimization Algorithm. *Mathematics* **2023**, *11*, 1298. https://doi.org/10.3390/math11061298

Academic Editors: Pedro Navas and Bo Li

Received: 7 February 2023
Revised: 25 February 2023
Accepted: 27 February 2023
Published: 8 March 2023

1. Introduction

1.1. Motivation

Over the last three decades, global warming has become a major issue for humanity. Indeed, the main responsibility is committed by the resources of fossil origin which are

currently ranked as the first sources of energy supply on a worldwide scale and which are becoming scarcer from one day to the next [1]. As such, developed and even developing countries are continuously adopting sustainable energy policies to achieve carbon dioxide (CO_2) emission reductions while ensuring a secure energy supply and a prosperous economy [2]. As a result, efforts have been intensified to promote the share of renewable energy to 30% by 2030. Recent studies have concluded that this target can even be exceeded towards achieving participation of RE in the global energy mix of about 36% if specific recommendations are properly addressed [3,4]. Among these recommendations, those related to the energy efficiency directive, improving access to energy, exploiting technological breakthroughs, consumer-driven societal developments, and the early retirement of conventional energy facilities, will effectively contribute to the achievement of such ecological and other goals [5].

Given the importance of the transport sector in the economic development of countries and its need for rapid economic expansion and urbanization as well as the necessity to improve people's livelihoods, the last few decades have been marked by a rapid increase in its energy consumption. This amounted to about 33% of the world's total, making it responsible for 37% of the total carbon dioxide emissions [6]. Faced with the serious environmental consequences of burning fossil fuels, the search for sustainable alternatives to provide energy in this sector becomes an urgent necessity. Therefore, one of the most relevant countermeasures is to shift the energy supply of the transport sector to renewable and clean energy sources, especially in oil-producing countries that depend mainly on it for consumption, such as the Kingdom of Saudi Arabia [7].

Within the framework of its Vision 2030 economic plan, the Saudi Commission for Tourism and National Heritage is working more and more to steadily increase the number of tourists visiting KSA. Therefore, the newest statistics of the World Tourism Organization (UNWTO) Tourism Barometer inform readers that KSA's tourism sector has risen rapidly to reach 121% compared to pre-COVID-19 pandemic international tourism.

In addition to religious tourism, desert tourism based primarily on electric vehicle (EV) transportation is a growing industry and a popular and sustainable option for exploring desert landscapes in the Hail region (HR) while reducing carbon emissions and noise pollution. Many tour agencies can offer electric vehicle tours, which makes the experience unique, enjoyable, and environmentally friendly since they can use zero-emission vehicles (ZEVs) including electric and hydrogen fuel cell vehicles [8].

Compared to combustion engines and electrochemical batteries, fuel cells are emerging as the most relevant choice in terms of environmental friendliness, durability, energy efficiency, autonomy and reliability [9–12]. In particular, proton exchange membrane fuel cells (PEMFCs) could be the leading candidate to power material handling applications and vehicles in the transportation sector [13].

1.2. Literature Review

Nowadays, PEMFCs are the best choice for future mobility and especially for hydrogen-powered vehicles. In order to master PEMFCs' operation and further push their development and efficiency, different modeling studies have been developed. A careful investigation allows for the classification of the analysis of PEMFCs in two main types of modeling, dynamic modeling, and steady-state modeling [14]. In this context, various published works have been focused on the PEMFCs modeling, control, and diagnosis to further advance their development and efficiency.

In [15], a real-time fault diagnostic/characterization of PEMFCs using a new concept combining a one-dimensional convolutional neural network and AC voltage response. For more complex applications, a diagnosis technique of faulty components of a 1 kW PEMFC-based system using energy analysis in [16]. In [17], a new robust estimator for the diagnosis and reconstruction of fault for a PEMFC air management system has been suggested under different conditions. The developed observer is able to accurately identify the state of the system even in case of any defects to achieve a tolerant control of the air

supply. In [18], the feasibility of a reliable method for the detection of abnormal sensors during PEMFC operation has been investigated. After their identification, the sensors identified as faulty are no longer considered in the diagnosis to guarantee the reliability of the PEMFC state of health monitoring. Particular attention was devoted to humidity sensors that can generate misleading readings regarding flooding. In [13], Chen et al. focused on the performance assessment and the thermodynamics–economy–environment feasibility of a PEMFC-based vehicle under dynamic conditions. In [19], the main objective has been devoted to the laboratory investigation of the effect of dynamic load cycle and operational parameters on the PEMFCs lifetime.

In addition to the previously mentioned studies, the accurate extraction of PEMFCs parameters remains crucial for improving their performance and durability as a promising technology for clean and efficient energy production. Recently, metaheuristic optimizers have been considered among the most used methods for tackling global optimization problems [20–23]. In this context, various optimization approaches have been proposed to address the PEMFCs parameters estimation issue. In [24], 18 optimization algorithms have been applied to estimate the parameters of three following practical fuel cells: BCS 500-W PEM, 500 W SR-12PEM, and 250 W PEMFC, under various operating conditions. Mohamed et al. [25] proposed a modified gorilla troops optimizer (MGTO) to tackle the drawbacks of the GTO such as the low speed of the convergence to local optima. The proposed approach has been tested to estimate the parameters of three types of PEMFCs. Otherwise, a honey badger optimizer (HBO) is used to identify the parameters of three commercial PEMFC by the minimization of the SSEs. Various metrics such as Sobol sensitivity and statistical study and computational complexity have been conducted to confirm the HBO performance [26]. Another recent study [27] has proposed to identify the PEMFC parameters using the original Bonobo Optimization algorithm (BO) and its enhanced version named Quasi Oppositional BO (QOBO). Otherwise, Ibrahim et al. [28] suggested identifying the design parameters of PEMFCs through an optimization algorithm called Enhanced Bald Eagle Search (EBES), under different pressure and temperature conditions. In [29], PEMFC parameters estimation based on a hybrid artificial bee colony differential evolution (ABCDE) optimizer has been suggested. The algorithm was tested, and the results showed that it can effectively estimate the parameters with high accuracy. Otherwise, a significant improvement has been applied to the African vulture optimizer [30] to investigate the parameter value estimation and fitting for NedStackPS6, BCS 500 W, and SR-12 500 W.

In the literature, the behavior of dandelions has been exploited by researchers, like various other biological phenomena and behaviors, to propose new optimization algorithms inspired by nature. A highly developed research has unveiled the first approach inspired by the behavior of dandelion sowing. This approach is commonly known as the Dandelion Algorithm (DA) [31]. Within the DA, the evolutionary process involves classifying the dandelion population into excellent and poor seeds based on their fitness values. Then, it retains the excellent seeds and assesses them to participate in the evolutionary process and excludes the poor seeds without any evaluation. From its first proposal, the DA has been investigated in an application related to the classification of biomedical problems by optimizing the input weights and output offsets of the extreme learning machine. In the same study, the major concern was associated with premature convergence to local optima. To overcome this limitation, a modified version was proposed for mutation-based seeding [32]. Correspondingly, the generation of mutation seeding is ensured upon a probability model exploiting Levy mutations and Gaussian mutations. The most significant improvement is provided by the evaluation of excellent seeds using the number of evaluations recorded after classifying seeds, discarding the bad ones, and taking into account only the excellent ones, which thereby considerably decreases the consumption of evaluations.

Furthermore, the Extreme Learning Machine (ELM) is known as a neural network algorithm (NNA) that generates, during the training process, input weights and offsets randomly and without dynamic adjustments [33]. Indeed, with only one parameter to

set (that materializes the hidden layer nodes), the ELM performs more efficiently and speedily than the traditional NNA. In order to benefit from its aforementioned strengths, ELM was proposed to take over the classification process and thus improve the dandelion DA algorithm (ELMDA) [34]. The fact that ELM's machine learning classifies dandelions into excellent and poor seeds according to their fitness and retains only the excellent ones motivates the evolution of the ELMDA algorithm.

Far from this theory and its applicability, a new concept inspired by the same natural phenomenon of a dandelion called Dandelion Optimizer (DO) has been investigated in the present work.

1.3. Contribution

The Dandelion Optimizer (DO) is a recent swarm intelligence bio-inspired optimizer developed by Zhao et al. [35]. It mimics the process of dandelion seeds' flight under the effect of the wind, to cross long distances. Such a process includes three main phases: ascent, descent, and landing. During the rising phase, the seeds drift along a localized community or spiral upwards under the effect of the whirlwinds deriving from the top to the ground. Then, according to the principles of Brownian motion and Levy's random walk, the seeds descend along a trajectory and land, respectively. Indeed, the flying seeds continue their descending by the adjustment of their trajectory in the global space and land at random to be able to grow again. The choice of the DO has been motivated by the fact that it has several strengths compared to other metaheuristic algorithms. These include:

- Low computational complexity: The evolution strategy used by the DO requires fewer computations than most other metaheuristic algorithms;
- Property of self-adaptation: The DO can self-adapt its parameters, allowing it to converge quickly and accurately to local minima and maximize the solution's performance;
- Minimization of stagnation of convergence: The DO utilizes a memory-based mechanism to identify stagnation of convergence and then takes steps to move away from a local minimum and towards a better solution;
- Ability to refer to an entire population: Unlike many other metaheuristic algorithms, the DO is able to refer to the entire population of solutions to best determine the optimal solution;
- Decentralized nature: The DO is a decentralized algorithm, meaning its components are distributed among multiple nodes or machines, making it less prone to failure than centralized algorithms.

The foremost contributions within the present work are:

- To adapt the DO algorithm, and benefit from its high exploitation and exploration abilities to address, for the first time, the issue of the PEMFC unidentified parameter estimation;
- Conducting a deep comparative study between DO and three recently published optimizers (Grey wolf optimizer (GWO), Gradient-based optimizer (GBO), and Harris hawks optimizer (HHO)) simulated under the same hypothesis;
- Comparing the DO performance with three competitive metaheuristic optimizers from the literature such as (Improved artificial ecosystem optimizer (IAEO), Vortex search-differential evolution (VSDE), and Artificial bee colony differential evolution shuffled complex (ABCDESC));
- The experimentation of two commercialized PEMFCs (EMFC 250 W, and NedStack PS6) has confirmed the superiority of the proposed DO in terms of stability, convergence speed, and absolute accuracy.

As shown in Figure 1, the proposed work design steps and flowchart are illustrated. Section 2 describes the mathematical modeling and the PEMFC; Section 3 formulates the investigated issue as an optimization problem; Section 4 discusses and analyses the main steps of the DO-based PEMFC parameter estimation; Section 5 is devoted to the validation of the DO, the discussions, and the comparative study with six well-known metaheuristic algorithms. Finally, the conclusions and future works are involved in Section 6.

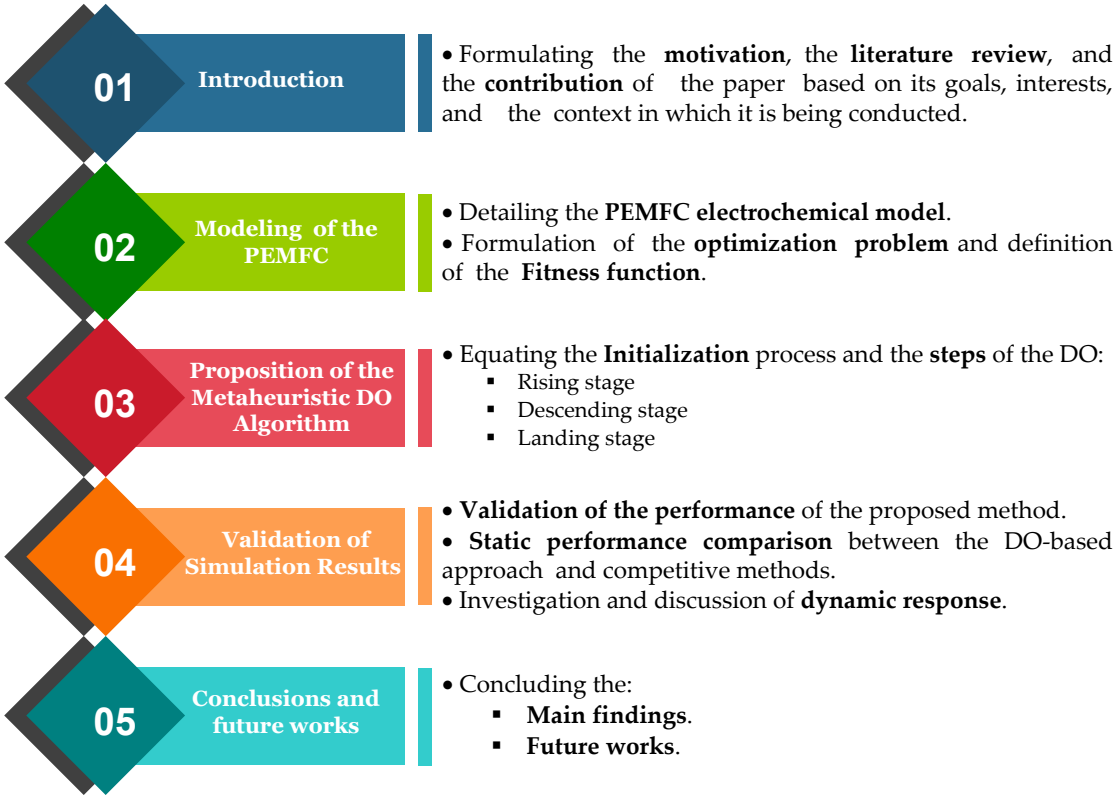

Figure 1. Flowchart illustrating the Research methodology .

2. General Model of PEM Fuel Cells

According to the literature, there are several types of models used to estimate the voltage–current relationship of the PEMFC. Amphlett's semi-empirical model is the most widely used thanks to its simplicity and efficiency [36,37]. In fact, this model presents the output voltage of a fuel cell as the sum of the thermodynamic Nernst voltage, the activation polarization, the concentration polarization, and the ohmic polarization (see Figure 2). Thus, the output voltage of the fuel cell can be written as Equation (1):

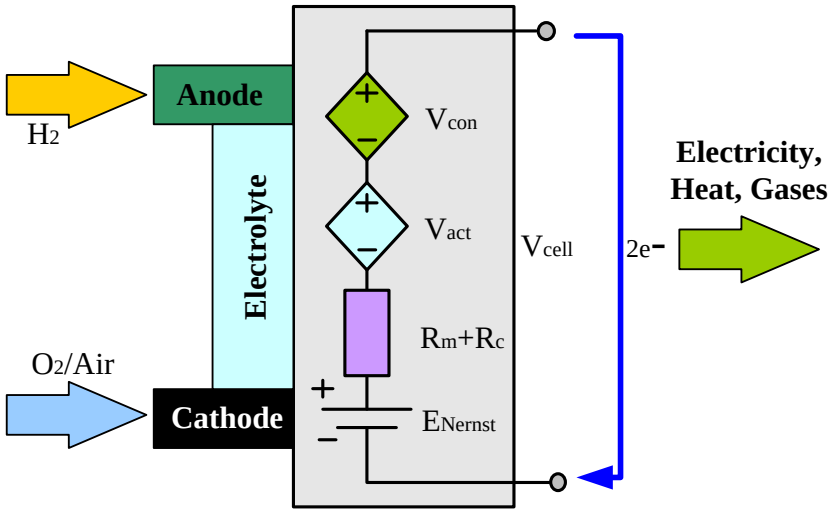

Figure 2. Electrical model of a PEM fuel cell.

$$V_{cell} = E_{Nernst} - V_{act} - V_{con} - V_{ohmic} \quad (1)$$

where V_{act} is the activation overpotential, V_{ohmic} is ohmic overpotential, V_{conc} denotes concentration loss, and E_{Nernst} is the theoretical voltage defined as follows [38–42]:

$$E_{Nernst} = 1.229 - 0.85 \times 10^{-3}(T - 298.15) + 4.308 \times 10^{-5} \times T \cdot \ln\left(P^*_{H_2}\sqrt{P^*_{O_2}}\right) \quad (2)$$

where T corresponds to the cell temperature at Kelvin, $P^*_{H_2}$ and $P^*_{O_2}$ are the partial pressures of hydrogen and oxygen, which may be calculated according to (3):

$$P^*_{H_2} = 0.5RH_a \cdot P^{sat}_{H_2O}\left[\frac{1}{\left(\frac{RH_a \cdot P^{sat}_{H_2O}}{P_a}\exp\left(\frac{1.635(i/A)}{T^{1.334}}\right)\right)} - 1\right] \quad (3)$$

$$P^*_{O_2} = RH_c \cdot P^{sat}_{H_2O}\left[\frac{1}{\left(\frac{RH_c \cdot P^{sat}_{H_2O}}{P_c}\exp\left(\frac{4.192(i/A)}{T^{1.334}}\right)\right)} - 1\right] \quad (4)$$

where RH_c and RH_a are the relative humidity at anode and cathode, P_a and P_c are the anode and cathode inlet pressures in atm, and $P^{sat}_{H_2O}$ is the saturation pressure of water vapor, obtained, in atm units, by the following formula:

$$\begin{aligned}\log_{10}(p^{sat}_{H_2O}) = 2.95 \times 10^{-2}\ (T - 298.15) - 9.18 \times 10^{-5}(T - 298.15)^2 \\ +1.44 \times 10^{-5}(T - 298.15)^3 - 2.18\end{aligned} \quad (5)$$

The activation losses V_{act} can be determined as in (6):

$$V_{\text{act}} = -\left[\xi_1 + \xi_2 T + \xi_3 T \ln\left(C_{O_2}\right) + \xi_4 T \ln(i)\right] \quad (6)$$

where ξ_1, ξ_2, ξ_4 and ξ_4 represent semi-empirical factors of cell model and C_{O_2} is the oxygen concentration can be calculated by:

$$C_{O_2} = \frac{P^*_{O_2}}{5.08} \times 10^{-6}\exp\left(\frac{498}{T}\right) \quad (7)$$

Next, the formulation for the calculation of ohmic losses used in this model is presented below:

$$V_{ohmic} = i(R_m + R_c) \quad (8)$$

The contact resistance at the terminals of the bipolar plates is denoted by R_c, and R_m represents the equivalent resistance of the membrane as follows:

$$R_m = \frac{\rho_m}{A} l_m \quad (9)$$

where l_m is the membrane thickness in cm, and ρ_m is the resistivity of membrane in $\Omega.cm$, defined as:

$$\rho_m = \frac{181.6\left[1 + 0.03 \times \left(\frac{i}{A}\right) + 0.062 \times \left(\frac{T}{303}\right)^2\left(\frac{i}{A}\right)^{2.5}\right]}{[\lambda_m - 0.634 - 3] \times \left(\frac{i}{A}\right)\exp\left[\frac{4.18\left(T^4 - 303\right)}{T}\right]} \quad (10)$$

where λ_m is an adjustable parameter that specifies membrane content the water.

Finally, the concentration losses can be established mathematically as in (11).

$$V_{con} = -b \cdot \ln\left(\frac{J_{max} - J}{J_{max}}\right) \tag{11}$$

where J is the current density (A cm^{-2}), and J_{max} is the maximum current density generated by the PEM fuel cell (A cm^{-2}). In the mathematical model of the PEM fuel cell, b is presented as an unknown coefficient.

In practice, fuel cells are stacked together in series to obtain higher power output. Depending on the number of cells, the output voltage of the stack V_{stack} is given by the following equation:

$$V_{stack} = N_{cell} \cdot V_{cell} \tag{12}$$

where N_{cell} number of cells in the stack.

3. Problem Formulation

The mathematical model of Amphlett [36,37] presents the nonlinear characteristics of the PEMFC stack. Since the implementation of an accurate model is a challenging task, this model depends on seven key variables. These adjustable variables are those used in the optimization problem to find the best solution for the objective function. The objective function defined in this study is the sum of squared errors (SSE). These errors quantify the difference between the voltage values, which are calculated mathematically, and those obtained from the voltage data measured in the laboratory from a real PEMFC. The mathematical description of this objective function is as follows:

$$F_{obj}\left(\xi_{i(1:4)}, \lambda_m, R_c, b\right) = \min\left(\sum_{j=1}^{N} \left(\mathrm{V_{mes}}(j) - \mathrm{V_{est}}(j)\right)^2\right) \tag{13}$$

Here, $\mathrm{V_{mes}}$ denotes the measured voltage of the PEMFC stack (V), $\mathrm{V_{est}}$ is the estimated voltage of the model (V), N is the number of measured data, and j is the counting factor. Depending on the type of the fuel cell and its operational state, b represents an empirical coefficient materializing the mass transport loss coefficient. The parameters of the PEMFC model are constrained by upper and lower boundaries that define the constraints of the problem in terms of inequality (14). The search ranges of ξ_i, λ_m, b and R_c are arranged in Table 1. These variables are those fitted by Dandelion Optimizer and some well-known algorithms.

$$\begin{aligned} \xi_i^{\min} &\le \xi_i \le \xi_i^{\max} \\ \lambda_m^{\min} &\le \lambda_m \le \lambda_m^{\max} \\ b^{\min} &\le b \le b^{\max} \\ R_c^{\min} &\le R_c \le R_c^{\max} \end{aligned} \tag{14}$$

Table 1. Parameter range of the PEMFC.

Parameter	ξ_1	ξ_2	ξ_3	ξ_4	λ_m	R_c	b
Min	-1.19969	1×10^{-3}	3.6×10^{-5}	-2.6×10^{-4}	10	1×10^{-4}	0.0136
max	-0.8532	5×10^{-3}	9.8×10^{-5}	-9.54×10^{-4}	24	8×10^{-4}	0.5

4. Proposed DO-Based Approach

Having previously explained the general concept of the DO algorithm, the next section focuses on the mathematical formulation of the three steps crossed by the dandelion seeds during their lifetime journey, namely the rising, the descending, and the landing.

4.1. Initialization

Having the same principle as that of the metaheuristic algorithms inspired by nature, the proposed algorithm is based on the initialization of the population through its evolution and iterative optimization. Indeed, each seed of dandelion can be considered as a candidate solution. According to this, the population can be represented by the matrix representation (Equation (15)):

$$Pop = \begin{bmatrix} x_{1,1} & x_{1,2} & \cdots & x_{1,D} \\ x_{2,1} & x_{2,2} & \cdots & x_{2,D} \\ \vdots & \vdots & \ddots & \vdots \\ x_{NP,1} & x_{NP,2} & \cdots & x_{NP,D} \end{bmatrix} \tag{15}$$

Herein, D is the variable dimension. NP represents the size of the population.

By defining two boundary bands to the treated problem: an upper and a lower one, denoted Ub and Lb respectively, as shown in these equations:

$$\begin{cases} Ub_j = [ub_1, \cdots, ub_D] \\ Lb_j = [lb_1, \cdots, lb_D] \end{cases} \tag{16}$$

Here, j is an integer between 1 and NP. Any candidate solution is necessarily being generated at random between such boundaries so that each individual $X_{i,j}$ is expressed according to Equation (17):

$$x_{i,j} = Lb_j + rand \cdot \left(Ub_j - Lb_j\right) \tag{17}$$

$rand$ is a random number between 0 and 1.

During the initialization process, the algorithm starts by choosing the individual having the optimal fitness value. After locating it, it is regarded as the initial elite that approximates the best location for the flourishing of the seed of dandelion. If the minimum value is chosen, the initial elite x_{elite} can be expressed as:

$$\begin{cases} F_{best} = \min\left(F_{obj}(x_{i,j})\right) \\ x_{elite} = x\left(find\left(F_{best} == F_{obj}(x_{i,j})\right)\right) \end{cases} \tag{18}$$

with $find()$ being two equal indices.

4.2. Rising Stage

During the rising phase, the dandelion seed rises to a specific height and then moves away from its parent. Subsequently, depending on moisture factors and wind strength, the seeds mount to random heights according to two weather conditions.

- **Condition 1** :
  On clear days without weather fluctuations, the wind speed is characterized by what can be modeled by a logarithmic distribution according to Equation (19):

$$lnY = N(\mu, \sigma^2)) \tag{19}$$

  Under these conditions, the transmission by seeds is remote randomly because the distribution is mainly along the y-axis, which triggers the process of DO exploration. In the search area, the dispersion of dandelion seeds is closely matched to the wind speed, which influences their height and dispersion. Under this impact, the vortices above the seeds are continuously adjusted to force them to spiral upward, according to the following equation:

$$X_{t+1} = X_t + \alpha \cdot v_x \cdot v_y \cdot \ln Y \cdot (X_s - X_t) \tag{20}$$

X_t and X_s denote the location of the dandelion seed and that of the search space for the iteration number t, respectively. As such, the location obtained by random is expressed by:

$$X_s = rand(1, \dim)(Ub - Lb) + Lb \tag{21}$$

It is important to mention that lnY is a lognormal distribution obeying the conditions $\sigma^2 = 1$ and $\mu = 0$, and so mathematically translated as:

$$\ln Y = \begin{cases} \frac{1}{y\sqrt{2\pi}} \exp\left[-\frac{1}{2\sigma^2}(\ln y)^2\right] & y \geq 0 \\ 0 & y \prec 0 \end{cases} \tag{22}$$

α is an adjustment parameter to adapt the search step length, and y is defined as the normal standard distribution $N(0, 1)$. Accordingly, α is given by:

$$\alpha = rand() * \left(\frac{1}{T^2}t^2 - \frac{2}{T}t + 1\right) \tag{23}$$

It was shown in [35] that the parameter α behaves as a function of the number of iterations as a random fluctuation in the range [0, 1] that decreases nonlinearly toward 0. When defining v_x and v_y as the dandelion lift parameter coefficients under the effect of the whirlwind action, the force calculation on the variable dimension obeys:

$$\begin{cases} r = \frac{1}{e^{\theta}} \\ v_x = r * \cos\theta \\ u_y = r * \sin\theta \end{cases} \tag{24}$$

where θ denotes a random angle in the interval $[-\pi, \pi]$.

- **Condition 2**:
  During rainy days, the air resistance is increased due to the high humidity, and therefore the buoyancy of dandelion seeds and their height in space are restricted, which involves the need to process it in their local proximities, according to the following equation Equation (25):

$$X_{t+1} = X_t * k \tag{25}$$

where k defines the parameter responsible for setting the local search domain of a given dandelion and which is assessed by Equation (26):

$$\begin{cases} q = \left(\frac{1}{T^2-2T+1}t^2 - \frac{2}{T^2-2T+1}t + 1 + \frac{1}{T^2-2T+1}\right) \\ k = 1 - rand() * q \end{cases} \tag{26}$$

At this stage, the seeds that are undergoing the rising phase are approximated by Equation (27):

$$X_{t+1} = \begin{cases} X_t + \alpha * v_x * v_y * \ln Y * (X_s - X_t) & rand(n) \prec 1.5 \\ X_t * k & else \end{cases} \tag{27}$$

4.3. Descending Stage

With the careful attention that the DO pays to the process of exploration, the descending phase is governed in accordance with the following analysis reflected by Equation (28). The dandelion seeds, being at the end of their rising phase to a certain distance, start the phase of regular descent according to a moving trajectory approximated by Brown's motion. Such normally distributed motion with each change enables individuals to cross, through the process of iterative updating, growing search communities. In a further phase, the optimizer expands the whole population to promising communities considering the average

location information after the ascension phase and all this for simulating the stability of the dandelion descending:

$$X_{t+1} = X_t - \alpha * \beta_t * (X_{mean\_t} - \alpha * \beta_t * X_t) \tag{28}$$

where β_t stands for a randomly generated number derived from the famous standard normal distribution and represents the Brownian movement. At the ith iteration, X_{mean_t} refers to the average population location according to Equation (29):

$$X_{mean\_t} = \frac{1}{pop} \sum_{i=1}^{pop} X_i \tag{29}$$

4.4. Landing Stage

The key to the successful implementation of metaheuristic algorithms is the balance between the two main search mechanisms, namely exploration and exploitation. In this context, the DO attempts, during the exploitation, to refine solutions already obtained during the exploration, to improve its fitness by searching the neighborhood of a promising region. The dandelion seeds land randomly in an unspecified location. However, as the iterations proceed, the algorithm converges to a globally optimal solution that pinpoints the approximate position that ensures the dandelion seeds germinate and continue their life cycle by borrowing the most relevant information from the actual elite by the search agents to exploit in their local neighborhoods. Assuming that, for the ith iteration, X_{elite} identifies the seed optimal position, the corresponding mathematical expression is as follows:

$$X_{t+1} = X_{elite} + levy(\lambda) * \alpha * (X_{elite} - \delta * X_t) \tag{30}$$

Herein, $levy(\lambda)$ denotes the Levy flight function given by:

$$levy(\lambda) = s \times \frac{w \times \sigma}{|t|^{\frac{1}{\beta}}} \tag{31}$$

The parameter β has been chosen randomly to equal 1.5, while s is fixed at 0.01 [35]. w and t are numbered in the interval [0, 1]. Accordingly, σ can be mathematically expressed by:

$$\sigma = \left(\frac{\Gamma(1+\beta) \times \sin\left(\frac{\pi\beta}{2}\right)}{\Gamma\left(\frac{1+\beta}{2}\right) \times \beta \times 2^{\left(\frac{\beta-1}{2}\right)}} \right) \tag{32}$$

Based on the previous value of β, σ increase linearly obeys Equation (33):

$$\delta = \frac{2t}{T} \tag{33}$$

4.5. Pseudo Code of the Proposed DO Algorithm

The Pseudo code of the proposed DO algorithm for PEMFC parameters estimation is summarized by Algorithm 1.

Algorithm 1 Pseudo-code of the proposed DO optimizer

Input: NP, T, D and measured V-I data
Output:$\boldsymbol{X_{best}}$ and $\boldsymbol{F_{best}}$
Initialize the initial dandelion seeds population in random way
Calculate the dandelion seeds fitness values $\boldsymbol{f}$
Choose $\boldsymbol{X_{elite}}$ based on the fitness value $\boldsymbol{f}$
while ($t < T$) **do**
  if $(rand() < 1.5)$ **then**
    Produce adaptive parameters using Equation (23)
    Update dandelion seeds by Equation (20)
    adaptive parameters using Equation (26)
    Update seeds by Equation (25)
  Update seeds by Equation (28)
  Update seeds by Equation (30)
  Arrange dandelion seeds based on fitness values
  Update $\boldsymbol{X_{elite}}$
  if $(f_{elite} = f(X_{best}))$ **then**
    $\boldsymbol{X_{Best}} = \boldsymbol{X_{elite}}$, $f_{Best} = f(X_{elite})$
Return $\boldsymbol{X_{Best}}$ and $\boldsymbol{F_{best}}$

5. Validation of Simulation Results

5.1. Identification of PEMFCs' Stack Parameters, Performance Measures and Comparisons

For a sufficiently rigorous validation, the proposed method is experimentally tested on two PEMFCs (PEMFC 250 W and NedStack PS6) whose electrical characteristics and operating conditions are shown in Table 2. The experimental data for the battery voltage versus the current are shown in [40] for different operating conditions. In addition, the DO Optimizer is compared with some well-functioning and competitive algorithms such as Harris Hawks Optimization (HHO), Grey Wolf Optimizer (GWO), and Gradient-based optimizer (GBO) through various statistical criteria such as accuracy, reliability, robustness, and stability. For a proper comparison, all of these algorithms were executed according to the same operating conditions, with the number of populations (N) fixed at 30 and the maximum number of iterations defined as 100. The best results of each algorithm are obtained after 30 executions. The simulations were performed using a Matlab 2019b environment on a laptop computer with an Intel Core i7-3630, 2.4 GHz processor, and 8 GB of RAM.

To further deepen the comparisons and prove the performance of the DO algorithm, its achieved results were also compared with those reached by three optimization methods well-cited in the literature such as improved artificial ecosystem optimizer (IAEO) [38], hybrid vortex search algorithm (VSDE) [39], and artificial bee colony differential evolution shuffled complex (ABCDESC) [40].

Table 2. The known parameters of PEMFCs.

Parameters	N_{cell}	A(cm^2)	l_m(μm)	J_{max}(A cm^2)	P_{H2}(bar)	P_{O2}(bar)	P_a(atm)	P_c(atm)	T(K)	P(kW)
250 W	24	27	127	0.86	3	5	-	-	353.15	0.25
NedSstack	65	240	178	1.2	-	-	1	1	343	6

The fitness function convergence curves of the different algorithms are shown for the two PEMFCs in Figure 3. In this figure, the convergence curve of the proposed DO algorithm reveals that it is much faster than the other three algorithms for the two investigated stacks. In both examples, the DO algorithm is computationally efficient, as it converges after a small number of iterations (27 iterations).

Tables 3 and 4 contain, respectively, the optimal parameters of the PEMFC 250 W and NedStack PS6 models estimated by the proposed DO and the other investigated algorithms.

To examine the superiority of the proposed DO, statistical measures, namely, best, worst, mean and standard deviation, are performed using the best fitness values obtained by each of the independent runs. Tables 3 and 4 summarize the values obtained for the two studied PEMFCs. It is worth highlighting that the proposed DO achieves the best value (0.158400329 PEMFC 250 W and 2.257565321 NedStack PS6) of the sum of square errors (SSE) as well as the lowest standard deviation (0.002660149 for PEMFC 250 W and 0.076297062 for NedStack PS6) compared to the other algorithms. The statistical results show that DO is consistent (in terms of robustness and efficiency) as the mean and standard deviation of SSE during 30 runs are lower than those obtained by the other algorithms for the two examined stacks.

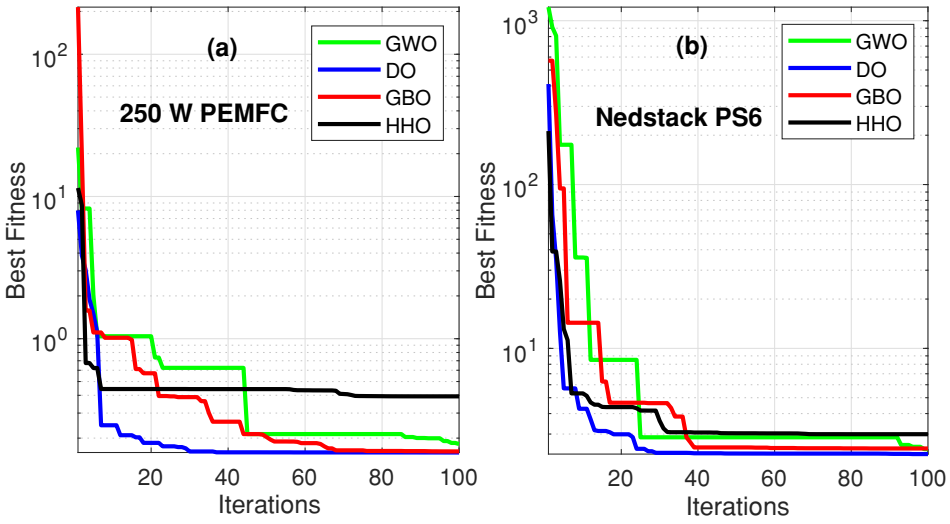

Figure 3. Convergence curve of fitness function: (**a**) 250 W fuel cell; (**b**) NedStack PS6 fuel cel.

Table 3. Optimal parameters of PEMFC 250 W.

Parameters	DO	GWO	GBO	HHO
ξ_1	−0.961592	−0.871596	−0.974457	−0.895253
ξ_2	0.00253443	0.00255737	0.00334035	0.00232372
ξ_3	3.6×10^{-5}	5.90919×10^{-5}	9.77117×10^{-5}	3.60984×10^{-5}
ξ_4	−0.000138245	−0.000141236	−0.000136735	−0.000100082
λ_m	13.3372	13.3735	13.9459	10.0273
R_c	0.000423201	0.000136504	0.0007994	0.000100273
b	0.0149649	0.0157339	0.0148931	0.0136372
Minimum SSE	0.158400329	0.160086164	0.158527784	0.276840933
Maximum SSE	0.166811864	0.353987785	0.272967021	2.136931329
Average SSE	0.160609673	0.194413051	0.18248663	0.983809404
Std SSE	0.002660149	0.046728642	0.033055337	0.488586136

Table 4. Optimal parameters of NedStack PS6.

Parameters	DO	GWO	GBO	HHO
ξ_1	−1.10823	−0.981556	−1.19841	−0.8532
ξ_2	0.00348488	0.0029638	0.00435526	0.00274411
ξ_3	5.23328×10^{-5}	4.10262×10^{-5}	9.40149×10^{-5}	5.17837×10^{-5}
ξ_4	-9.54×10^{-5}	-9.55047×10^{-5}	-9.54×10^{-5}	-9.54×10^{-5}
λ_m	23.0714	14.9218	23.95	14.3893
R_c	0.000127527	0.000198012	0.000327086	0.000186993
b	0.0835662	0.0236393	0.0539602	0.0195792

Table 4. *Cont.*

Parameters	DO	GWO	GBO	HHO
Minimum *SSE*	2.077565321	2.288386949	2.278642183	2.286126251
Maximum *SSE*	2.627548699	4.705647651	3.756412117	9.447348766
Average *SSE*	2.501037792	3.038447633	2.873919639	4.517318823
Std *SSE*	0.076297062	0.618991833	0.248397126	1.865763408

In order to evaluate the stability of the different algorithms, the boxplots, for the SSE after 30 repetitions of 100 iterations, are plotted in Figures 4 and 5. The interquartile ranges increase as one moves from the DO algorithm to the GBO algorithm and then GWO and HHO. The distribution of outcomes (SSE) built by the DO algorithm is around its median. Based on these comparisons, it can be concluded that the proposed DO algorithm achieves better performance in terms of accuracy and robustness compared to the other algorithms.

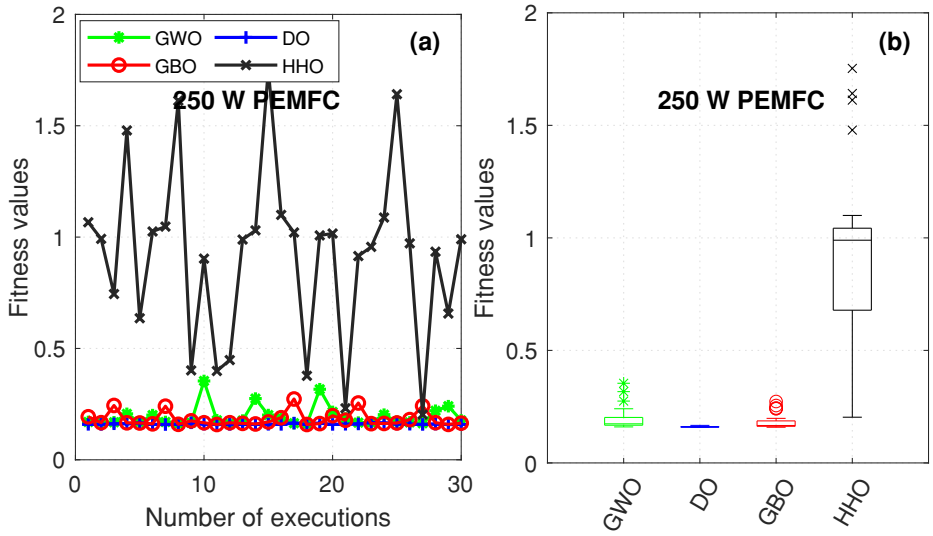

Figure 4. The statistical study of the 250 W after 30 repetitions: (**a**) best values of the objective function; (**b**) boxplot of SSE.

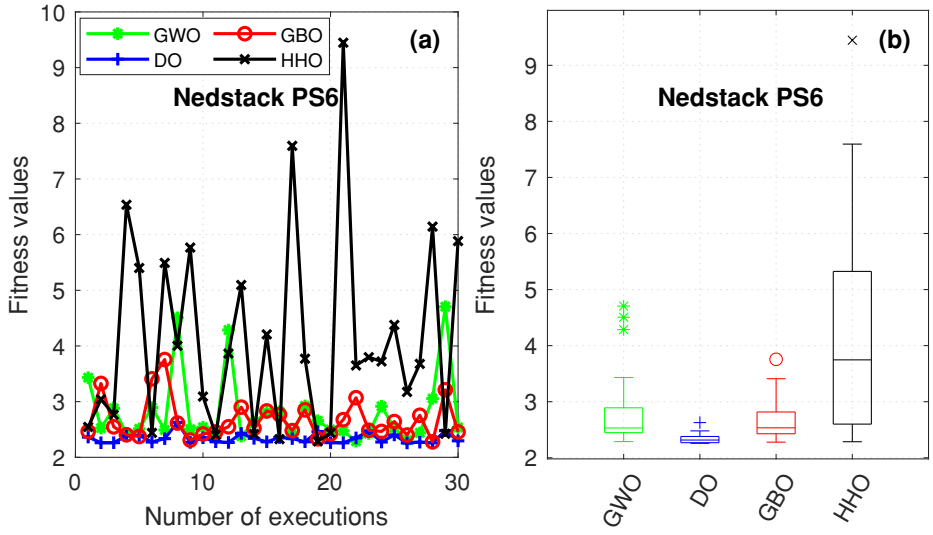

Figure 5. The statistical study of the NedStack PS6: (**a**) best values of the objective function; (**b**) boxplot of SSE.

Tables 5 and 6 summarize the results of the DO, IAEO, VSDE, and ABCDESC algorithms by illustrating the estimated parameters and SSE metric of the experimented PEMFC 250 W and NedStack PS6 fuel cells. In both case studies, the proposed DO algorithm reaches the best results with minimum SSE compared with other algorithms.

Table 5. Optimum values of unknown parameters and SSE of PEMFC 250 W.

Parameters	DO	IAEO [18]	VSDE [39]	ABCDESC [40]
ξ_1	-0.961592	-0.9991	-1.1921	-1.12806
ξ_2	0.00253443	0.002825	0.0031990	0.00394667
ξ_3	3.6×10^{-5}	4.47×10^{-5}	3.799×10^{-5}	9.777204×10^{-5}
ξ_4	-0.000138245	-0.00017	-0.000187	-0.000174889
λ_m	13.3372	19.99358	22.817	19.9358326
R_c	4.23201×10^{-4}	1.000×10^{-4}	1.202×10^{-4}	1×10^{-4}
b	0.0149649	0.0145	0.0290	0.014526
Minimum SSE	0.158400329	0.3360	1.0526	0.33597

Table 6. Optimum values of unknown parameters and SSE of NedStack PS6.

Parameters	DO	IAEO [18]	VSDE [39]	ABCDESC [40]
ξ_1	-1.10823	-0.9822	-1.1212	-0.9350526
ξ_2	0.00348488	0.0035957	0.00033487	0.0035035
ξ_3	5.23328×10^{-5}	9.48×10^{-5}	4.6787×10^{-5}	9.793216×10^{-5}
ξ_4	-9.54×10^{-5}	-9.54×10^{-5}	-9.5400×10^{-5}	-9.54×10^{-5}
λ_m	23.0714	13.4650	13.0000	13.094707
R_c	1.27527×10^{-4}	1.00×10^{-4}	1.00×10^{-4}	0.0001
b	0.0835662	0.0136	0.0494	0.0136
Minimum SSE	2.077565321	2.1459	2.088	2.079204604

Figures 6 and 7 show the experimental polarization curves and the best polarization curves obtained through the model of the I–V and I–P characteristics of the two studied PEMFCs. A closer examination of these graphs shows that the simulation results of the model with the parameters estimated using the proposed DO are very close to the experimental results. This further emphasizes the superiority of the DO to achieve a very accurate model.

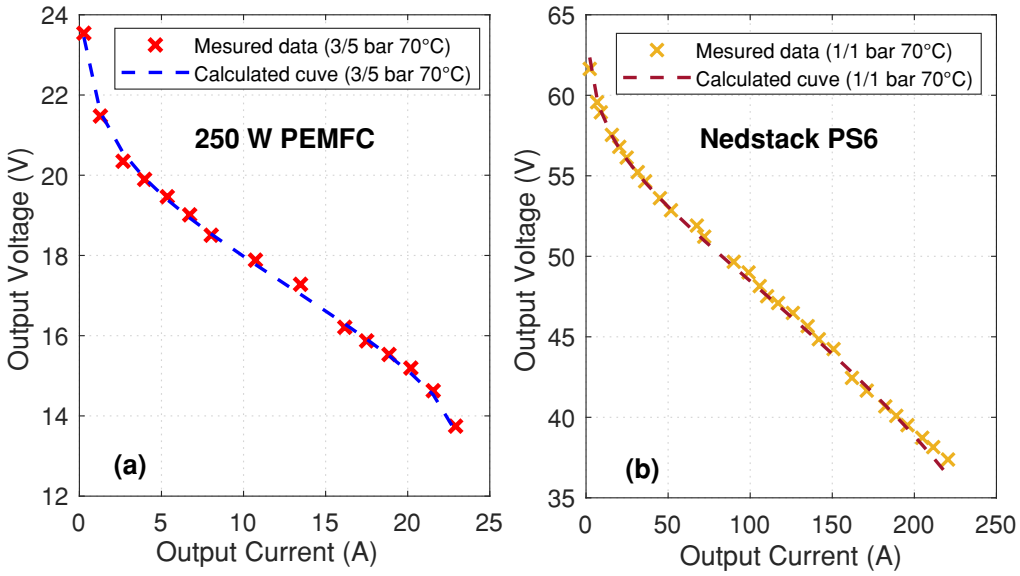

Figure 6. The current–voltage curve: (**a**) 250 W fuel cel; (**b**) NedStack PS6 fuel cell.

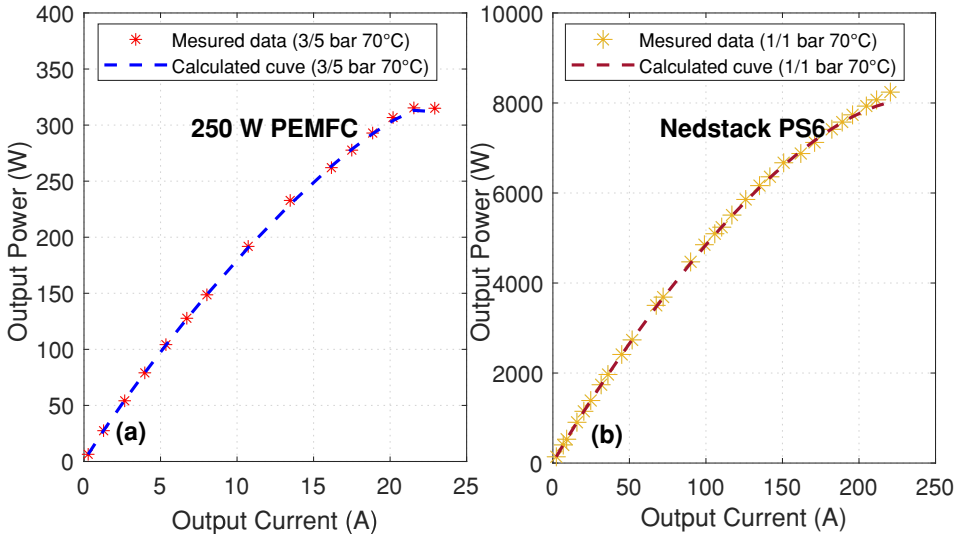

Figure 7. The current–power curve: (**a**) 250 W fuel cell; (**b**) NedStack PS6 fuel cell.

The absolute deviation of each voltage point between the real and estimated data $Div = V_{mes} - V_{est}$ of the two stacks (250 W PEMFC and NedStack PS6) for the best results of all 30 independent tests is displayed in Tables 7 and 8.

Table 7. Estimated voltage and absolute deviation of the 250 W PEMFC.

N	$i(A)$	$V_{mes}(V)$	$V_{est}(V)$	$Div(V)$	$(Div)^2(V)$
1	0.2729	23.5410	23.436884	0.1041	0.0108
2	1.2790	21.4756	21.552742	−0.0771	0.0060
3	2.6603	20.3484	20.542713	−0.1943	0.0378
4	3.9734	19.8969	19.913082	−0.0162	2.6186×10^{-4}
5	5.3547	19.4642	19.385395	0.0788	0.0062
6	6.7190	19.0127	18.934608	0.0781	0.0061
7	8.0321	18.5049	18.470406	0.0345	0.0012
8	10.7265	17.8835	17.792614	0.0909	0.0083
9	13.4720	17.2808	17.135401	0.1457	0.0449
10	16.1664	16.2089	15.996914	0.2120	0.0212
11	17.4966	15.8701	15.988641	−0.1185	0.0141
12	18.8608	15.5312	15.594024	−0.0628	0.0039
13	20.1910	15.1923	15.175456	0.01686	2.8372×10^{-4}
14	21.5553	14.6282	14.586637	0.0416	0.0017
15	22.9195	13.7450	13.693124	0.0519	0.0027
SSE	0.158400329				

Table 8. Estimated voltage and absolute deviation of the NedStack PS6.

N	$i(A)$	$V_{mes}(V)$	$V_{est}(V)$	$Div(V)$	$(Div)^2(V)$
1	2.25	61.64	62.452443	−0.8124	0.6600
2	6.75	59.57	59.873841	−0.3038	0.0923
3	9.00	58.94	59.140399	−0.2003	0.4877
4	15.75	57.54	57.582298	−0.04229	0.0017
5	20.25	56.80	56.799747	0.0002	6.36×10^{-8}
6	24.75	56.13	56.122583	0.0074	5.5×10^{-5}
7	31.50	55.23	55.729928	0.0003	1.37×10^{-7}
8	36.00	54.66	54,589203	0.0707	0.0050
9	45.00	53.61	53.604175	0.0058	3.39×10^{-5}
10	51.75	52.86	52,799762	0.0602	0.0036

Table 8. *Cont.*

N	$i(A)$	$V_{mes}(V)$	$V_{est}(V)$	$Div(V)$	$(Div)^2(V)$
11	67.50	51.91	51.48410	0.4258	0.1813
12	72.00	51.22	51.068878	0.1511	0.0228
13	90.00	49.66	49,452415	0.2075	0.04309
14	99.00	49.00	48.659847	0.3401	0.1157
15	105.80	48.15	48.064054	0.0859	0.0073
16	110.30	47.52	47.670360	−0.1503	0.0022
17	117.00	47.10	47.084098	0.0159	0.0002
18	126.00	46.48	46.294582	0.1854	0.0343
19	135.00	45.66	45.500518	0.1594	0.0254
20	141.80	44.85	44.799173	0.0508	0.0025
21	150.80	44.24	44,088817	0.1511	0.0228
22	162.00	42.45	43.069394	−0.6193	0.3836
23	171.00	41.66	42,235973	−0.5759	0.3317
24	182.30	40.68	40.708183	−0.0281	0.0007
25	189.00	40.09	40.102165	−0.0121	0.0001
26	195.80	39.51	39.455396	0.0546	0.0.0030
27	204.80	38.73	38.553613	0.1763	0.0311
28	211.50	38.15	38.696963	0.1837	0.0337
29	220.50	37.38	37.18800	0.1919	0.0368
SSE	2.257565321				

The previous results prove the excellent agreement between the measured voltage data of the two stacks (250 W PEMFC and NedStack PS6) and the model data found by the DO-based method. This is once again significant proof of the exactitude of the seven parameter values of the PEMFCs identified by DO.

5.2. Transient Response to Current Changes

The changing of the current level induces a variation of the cell voltage. Indeed, if the current varies, a time delay is required for the cell voltage to reach its steady-state value. This delay clearly affects the activation and concentration drops. However, the ohmic potential is not sensitive to this delay. To provide an approximate representation of this phenomenon, a first order transfer function cascaded with the activation and concentration potentials is adopted. In such a situation, Equations (6) and (11) are rewritten as indicated, respectively, in Equations (34) and (35):

$$V_{\text{act}} = -\left[\xi_1 + \xi_2 T + \xi_3 T \ln\left(C_{O_2}\right) + \xi_4 T \ln(i)\right] \cdot \frac{1}{1 + T_r \cdot s} \tag{34}$$

$$V_{con} = -b \cdot \ln\left(\frac{J_{max} - J}{J_{max}}\right) \cdot \frac{1}{1 + T_r \cdot s} \tag{35}$$

Herein, T_r represents the transfer function time constant.

The dynamic model is depicted in the diagram of Figure 8. It is worth mentioning that pressures, thermodynamics and valve handling are not considered in this simplified dynamic model. As illustrated in the figure, the irreversible voltage losses in the PEMFC are obtained via the "PEMFC voltage losses model" block, taking into consideration the response time of the stack. The open circuit voltage is represented by the "PEMFC Nernst output voltage model" block. It is important to remember that this voltage is determined by applying Equation (2).

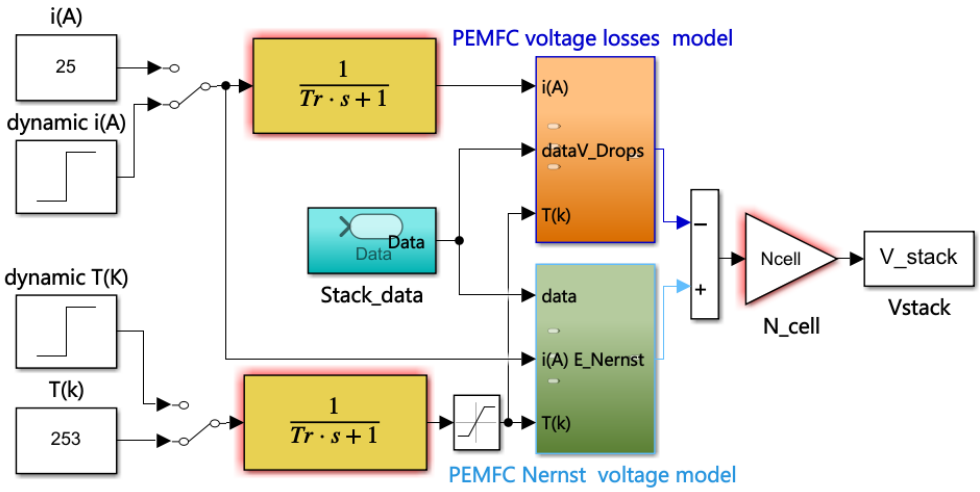

Figure 8. PEMFC simplified dynamic model.

In order to evaluate the degree of compatibility of the model based on the DO algorithm to the actual behavior of the stack, the NedStack PS6 stack is chosen to simulate the dynamic response due to changes in load current. Thus, the model based on the GBO algorithm, which has a better SSE compared to the other two methods (GWO and HHO), is simulated to perform such a comparison. Table 6 presents the best values of the unknown parameters obtained by the DO compared to those obtained by the GBO.

The experimental I–V characteristic as well as those obtained using the simulated BO-based model and the GBO-based model are depicted in Figure 9a. The results obtained are in full agreement with those shown previously; the plots show a good fit between the experimental I–V characteristics and those derived from the BO and GBO-based models. To investigate further, the unknown parameter values obtained are used in the dynamic model implemented in MATLAB/SIMULINK to examine the dynamic performance of the PS6 stack in the case where *Tr* equals 3 s.

To obtain an idea about the dynamic performance of the fuel cell, two load variation scenarios are applied to the generated model (increase and decrease) as shown in Figure 9b. The assumed increase and decrease time instants are 30 s and 60 s, respectively. Figure 9c shows the dynamic responses of the NedStack PS6 battery voltage as a function of load current variations. It is meaningfully clear that both models exhibit transient responses to these changes. As the load current increases, the stack voltage decreases until it reaches its steady-state value, as illustrated by the curves in Figure 9a,c.

On the other hand, when the current decreases, the stack reacts again to this change and, after a short time, the stack voltage rejoins the value of its steady-state voltage. In both cases, the performances shown are very satisfactory.

This is also confirmed by Figure 9d where the voltage errors between the real model and those generated from the BO and GBO-based models. It is shown in this figure that the voltage error generated by the developed DO model is lower.

In contrast to the optimization algorithms and the difficulties that can be encountered in their implementation for solving engineering problems, the implementation of the DO algorithm for extracting the unknown parameters of the PEMFC model allowed us to achieve the foregoing:

- Regarding the parameter settings, the population size, the mutation rate and the convergence criteria have been set appropriately for the present problem without any difficulties to be mentioned;
- For the implementation complexity, the complex operations involved in the whole process, i.e., the rising, descending, and landing stages, and the steps of generating the seeds and updating them, etc., the simplicity of the DO has allowed its implementation to be successful;

- Concerning memory usage, the dimensionality of the solved optimization problem did not cause any problems in this respect;
- The convergence speed of the DO has been satisfactory since it runs for a short period of time and achieves better results than the other tested algorithms.

Overall, with careful consideration and appropriate attention to the processes of the DO algorithm, its implementation to address the current research problem has achieved good results. Nevertheless, the concerns that may be raised will obviously be related to the cases of more complex and challenging problems with higher dimensionalities, requiring a larger amount of memory, and/or a longer execution period.

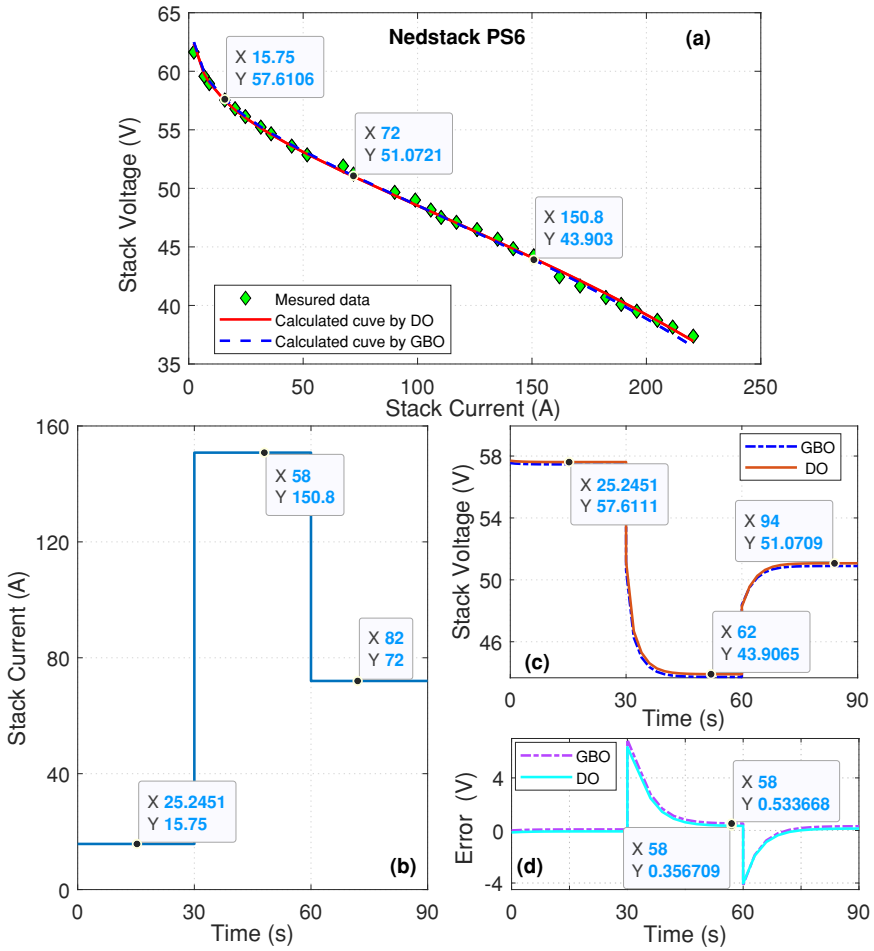

Figure 9. Characteristic and dynamic simulations of the PS6 stack: (**a**) I–V polarisation; (**b**) stack load current changes; (**c**) stack voltage responses; (**d**) voltage error.

6. Conclusions and Future Works

The research work presented in this paper deals with the development of a new optimization approach based on the DO algorithm to effectively address the (theoretical) problem of identifying the key parameters of the PEMFCs. The objective function presented aims to minimize the sum of squared deviations between the generated theoretical model and the experimental measurements of two PEM fuel cells, namely PEMFCs 250 W stack and NedStack PS6. The seven variables to be approximated are the following: ξ_1, ξ_2, ξ_3, ξ_4, λ_m, b and R_c. According to the proposed Do features, the results of its performance analysis are compared with several other programmed meta-heuristic approaches and others reported from the literature namely GWO, GBO, HHO, IAEO, VSDE, and ABCDESC under the conditions imposed by the constraints of the variables to be estimated.

The series of conducted tests and experiments showed that the proposed algorithm obtains better results, in comparison with those obtained by the competitive algorithms.

Indeed, the DO approach is faster than the other approaches in terms of generated outcomes for two tested stacks. Otherwise, it also obtained better solutions than the other methods, which shows the efficiency and robustness of the implemented approach. The superiority and efficiency of the DO are evident in terms of maximum, minimum, and median for the tested piles.

Although the performance of the proposed approach is significantly promising as a valuable tool, used for the first time, for solving the problem of nonlinear fuel cell model equations and estimating its unknown parameters, future recommendations are mainly targeted to its improvement and exploitation in this application and other fields related to renewable energy and power systems.

Author Contributions: All authors (R.A., S.S., A.A., H.J., M.K. and B.N.A.) contributed equally. All authors have read and agreed to the published version of the manuscript.

Funding: This research has been funded by Scientific Research Deanship at the University of Ha'il, Saudi Arabia through project number RD-21 083.

Data Availability Statement: Not applicable.

Conflicts of Interest: The authors declare no conflict of interest.

Abbreviations

The following abbreviations are used in this manuscript:

PEMFC	Proton exchange membrane fuel cell
DO	Dandelion optimizer
GWO	Grey wolf optimizer
GBO	Gradient-based optimizer
HHO	Harris Hawks optimizer
IAEO	Improved artificial ecosystem optimizer
VSDE	Vortex search-differential evolution
ABCDESC	Artificial bee colony differential evolution shuffled complex
HR	Hail region
CO_2	Carbon dioxide
CO	Carbon monoxide
H_2O	Water molecule
H_2	Hydrogen gas
O_2	Dioxygen gas
RE	Renewable energy
KSA	Kingdom of Saudi Arabia
UNWTO	World Tourism Organization
COVID-19	Coronavirus disease
EV	Electric vehicle
ZEVs	Zero-emission vehicles
AC	Alternative current
GTO	Gorilla troops optimizer
MGTO	Modified GTO
HBO	Honey badger optimizer
SSE	Sum of squared errors
BO	Bonobo optimizer
QOBO	Quasi oppositional bonobo optimizer
EBES	Enhanced bald eagle search
DA	Dandelion algorithm
ELM	Extreme learning machine
NNA	Neural network algorithm
ELMD	Dandelion algorithm with ELM

References

1. Zhao, L.; Jerbi, H.; Abbassi, R.; Liu, B.; Latifi, M.; Nakamura, H. Sizing renewable energy systems with energy storage systems based microgrids for cost minimization using hybrid shuffled frog-leaping and pattern search algorithm. *Sustain. Cities Soc.* **2021**, *73*, 103124. [CrossRef]
2. Li, N.; Su, Z.; Jerbi, H.; Abbassi, R.; Latifi, M.; Furukawa, N. Energy management and optimized operation of renewable sources and electric vehicles based on microgrid using hybrid gravitational search and pattern search algorithm. *Sustain. Cities Soc.* **2021**, *75*, 103279. [CrossRef]
3. Alturki, M.; Abbassi, R.; Albaker, A.; Jerbi, H. A New Hybrid Synchronization PLL Scheme for Interconnecting Renewable Energy Sources to an Abnormal Electric Grid. *Mathematics* **2022**, *10*, 1101. [CrossRef]
4. Abbassi, R.; Marrouchi, S.; Ben Hessine, M.; Chebbi, S.; Juini, H. Voltage Control Strategy of an Electrical Network by the Integration of the UPFC Compensator. *Int. Rev. Model. Simul.* **2012**, *5*, 380–384.
5. Abbassi, R.; Hammami, M.; Chebbi, S. Improvement of the integration of a grid-connected wind-photovoltaic hybrid system. In Proceedings of the International Conference on Electrical Engineering and Software Applications, Yasmine Hammamet, Tunisia, 17–19 March 2013.
6. Hong, M.D.; Yun, P.Z.; Jing, L.; Wei, T.G.; Chu, J.B. Research on energy saving potential and countermeasures in China's transport sector. *Energy Rep.* **2022**, *8*, 300–311.
7. Marko, M.; Maja, P.; Nikola, V.; Goran, K. Cross-sectoral integration for increased penetration of renewable energy sources in the energy system – Unlocking the flexibility potential of maritime transport electrification. *Smart Energy* **2022**, *8*, 100089.
8. Rasul, M.G.; Hazrat, M.A.; Sattar, M.A.; Jahirul, M.I.; Shearer, M.J. The future of hydrogen: Challenges on production, storage and applications. *Energy Convers. Manag.* **2022**, *272*, 116326. [CrossRef]
9. Hong, S.; Lee, J.; Cho, H.; Kim, M.; Moon, I.; Kim, J. Multi-objective optimization of CO_2 emission and thermal efficiency for on-site steam methane reforming hydrogen production process using machine learning. *J. Clean. Prod.* **2022**, *359*, 132133. [CrossRef]
10. Yan, X.; Li, Y.; Sun, C.; Zhang, C.; Yang, L.; Fan, X.; Chu, L. Enhanced H_2 production from steam gasification of biomass by red mud-doped Ca-Al-Ce bi-functional material. *Appl. Energy* **2022**, *312*, 118737. [CrossRef]
11. Zhang, X.Y.; Yu, W.L.; Zhao, J.; Dong, B.; Liu, C.G.; Chai, Y.M. Recent development on self-supported transition metal-based catalysts for water electrolysis at large current density. *Appl. Mater. Today* **2021**, *22*, 100913. [CrossRef]
12. Matoba, K.; Takahashi, M.; Matsuda, Y.; Higashimoto, S. Photoelectrochemical water splitting on the Pt-In2S3/CuInS2 photoelectrode under solar light irradiation: Effects of electrolytes on the solar energy to hydrogen conversion. *J. Electroanal. Chem.* **2021**, *895*, 115489. [CrossRef]
13. Chen, X.; Long, S.; He, L.; Wang, C.; Chai, F.; Kong, X.; Wan, Z.; Song, X.; Tu, Z. Performance evaluation on thermodynamics-economy-environment of PEMFC vehicle power system under dynamic condition. *Energy Convers. Manag.* **2022**, *269*, 116082. [CrossRef]
14. Ouaidat, G.; Cherouat, A.; Kouta, R.; Chamoret, D. Study of the effect of mechanical uncertainties parameters on performance of PEMFC by coupling a 3D numerical multiphysics model and design of experiment. *Int. J. Hydrogen Energy* **2022**, *47*, 23772–23786. [CrossRef]
15. Zhou, S.; Tranter, T.; Neville, T.P.; Shearing, P.R.; Brett, D.J.; Jervis, R. Fault diagnosis of PEMFC based on the AC voltage response and 1D convolutional neural network. *Cell Rep. Phys. Sci.* **2022**, *3*, 101052. [CrossRef]
16. Seo, S.H.; Oh, S.D.; Park, J.; Park, J.Y.; Lim, I.S.; Kim, M.S.; Kwak, H.Y. Diagnosis of a hydrogen-fueled 1-kW PEMFC system based on exergy analysis. *Int. J. Hydrogen Energy* **2020**, *45*, 17745–17758. [CrossRef]
17. Yang, D.; Wang, Y.; Chen, Z. Robust fault diagnosis and fault tolerant control for PEMFC system based on an augmented LPV observer. *Int. J. Hydrogen Energy* **2020**, *45*, 13508–13522. [CrossRef]
18. Mao, L.; Jackson, L.; Davies, B. Investigation of PEMFC fault diagnosis with consideration of sensor reliability. *Int. J. Hydrogen Energy* **2018**, *43*, 16941–16948. [CrossRef]
19. Chu, T.; Xie, M.; Yu, Y.; Wang, B.; Yang, D.; Li, B.; Ming, P.; Zhang, C. Experimental study of the influence of dynamic load cycle and operating parameters on the durability of PEMFC. *Energy* **2022**, *239*, 122356. [CrossRef]
20. Tang, S.; Jiang, M.; Abbassi, R.; Jerbi, H. A cost-oriented resource scheduling of a solar-powered microgrid by using the hybrid crow and pattern search algorithm. *J. Clean. Prod.* **2021**, *313*, 127853. [CrossRef]
21. Guo, S.; Abbassi, R.; Jerbi, H.; Rezvani, A.; Suzuki, K. Efficient maximum power point tracking for a photovoltaic using hybrid shuffled frog-leaping and pattern search algorithm under changing environmental conditions. *J. Clean. Prod.* **2021**, *297*, 126573. [CrossRef]
22. Abbassi, A.; Abbassi, R.; Heidari, A.A.; Oliva, D.; Chen, H.; Habib, A.; Jemli, M.; Wang, M. Parameters identification of photovoltaic cell models using enhanced exploratory salp chains-based approach. *Energy* **2020**, *198*, 117333. [CrossRef]
23. Abbassi, R.; Abbassi, A.; Heidari, A.A.; Mirjalili, S. An efficient salp swarm-inspired algorithm for parameters identification of photovoltaic cell models. *Energy Convers. Manag.* **2019**, *179*, 362–372. [CrossRef]
24. Diab, A.A.Z.; Ali, H.; Abdul-Ghaffar, H.I.; Abdelsalam, H.A.; Abd El Sattar, M. Accurate parameters extraction of PEMFC model based on metaheuristics algorithms. *Energy Rep.* **2021**, *7*, 6854–6867. [CrossRef]
25. Abdel-Basset, M.; Mohamed, R.; Chang, V. An Efficient Parameter Estimation Algorithm for Proton Exchange Membrane Fuel Cells. *Energies* **2021**, *14*, 7115. [CrossRef]

26. Ashraf, H.; Abdellatif, S.O.; Elkholy, M.M.; El-Fergany, A.A. Honey badger optimizer for extracting the ungiven parameters of PEMFC model: Steady-state assessment. *Energy Convers. Manag.* **2022**, *258*, 115521. [CrossRef]
27. Sultan, H.M.; Menesy, A.S.; Hassan, M.S.; Jurado, F.; Kamel, S. Standard and Quasi Oppositional bonobo optimizers for parameter extraction of PEM fuel cell stacks. *Fuel* **2023**, *340*, 127586. [CrossRef]
28. Alsaidan, I.; Shaheen, M.A.; Hasanien, H.M.; Alaraj, M.; Alnafisah, A.S. A PEMFC model optimization using the enhanced bald eagle algorithm. *Ain Shams Eng. J.* **2022**, *13*, 101749. [CrossRef]
29. Hachana, O.; El-Fergany, A.A. Efficient PEM fuel cells parameters identification using hybrid artificial bee colony differential evolution optimizer. *Energy* **2022**, *250*, 123830. [CrossRef]
30. Yongguang C.; Guanglei Z. New parameters identification of Proton exchange membrane fuel cell stacks based on an improved version of African vulture optimization algorithm. *Energy Rep.* **2022**, *8*, 3030–3040.
31. Li, X.; Han, S.; Zhao, L.; Gong, C.; Liu, X. New dandelion algorithm optimizes extreme learning machine for biomedical classification problems. *Comput. Intell. Neurosci.* **2017**, *2017*, 4523754. [CrossRef]
32. Zhu, H.; Liu, G.; Zhou, M.; Xie, Y.; Kang, Q. Dandelion Algorithm With Probability-Based Mutation. *IEEE Access* **2019**, *7*, 97974–97985. [CrossRef]
33. Wang, J.; Lu, S.; Wang, S.H.; Zhang, Y.D. A review on extreme learning machine. *Multimed. Tools Appl.* **2022**, *81*, 41611–41660. [CrossRef]
34. Han, S.; Zhu, K.; Wang, R. Improvement of evolution process of dandelion algorithm with extreme learning machine for global optimization problems. *Expert Syst. Appl.* **2021**, *163*, 113803. [CrossRef]
35. Zhao, S.; Zhang, T.; Ma, S.; Chen, M. Dandelion Optimizer: A nature-inspired metaheuristic algorithm for engineering applications. *Eng. Appl. Artif. Intell.* **2022**, *114*, 105075. [CrossRef]
36. Daeichian, A.; Ghaderi, R.; Kandidayeni, M.; Soleymani, M.; Trovão, J.P.; Boulon, L. Online characteristics estimation of a fuel cell stack through covariance intersection data fusion. *Appl. Energy* **2019**, *292*, 116907. [CrossRef]
37. Nóbrega, P.H.A. A review of physics-based low-temperature proton-exchange membrane fuel cell models for system-level water and thermal management studies. *J. Power Sources* **2019**, *558*, 232585. [CrossRef]
38. Rizk-Allah, R.M.; El-Fergany, A.A. Artificial ecosystem optimizer for parameters identification of proton exchange membrane fuel cells model. *Int. J. Hydrogen Energy* **2021**, *46*, 37612–37627. [CrossRef]
39. Fathy, A.; Abd Elaziz, M.; Alharbi, A.G. A novel approach based on hybrid vortex search algorithm and differential evolution for identifying the optimal parameters of PEM fuel cell. *Renew. Energy* **2020**, *146*, 1833–1845. [CrossRef]
40. Hachana, O. Accurate PEM fuel cells parameters estimation using hybrid artificial bee colony differential evolution shuffled complex optimizer. *Int. J. Energy Res.* **2022**, *46*, 6383–6405. [CrossRef]
41. Fathy, A.; Rezk, H. Multi-verse optimizer for identifying the optimal parameters of PEMFC model. *Energy* **2018**, *143*, 634–644. [CrossRef]
42. Rezaie, M.; karamnejadi azar, K.; Sani, A.K.; Akbari, E.; Ghadimi, N.; Razmjooy, N.; Ghadamyari, M. Model parameters estimation of the proton exchange membrane fuel cell by a Modified Golden Jackal Optimization. *Energy Technol. Assess.* **2022**, *53 Pt C*, 102657. [CrossRef]